

Quantum spin liquids: a large-S route

This article has been downloaded from IOPscience. Please scroll down to see the full text article.

2004 J. Phys.: Condens. Matter 16 S709

(<http://iopscience.iop.org/0953-8984/16/11/019>)

View [the table of contents for this issue](#), or go to the [journal homepage](#) for more

Download details:

IP Address: 129.252.86.83

The article was downloaded on 27/05/2010 at 12:52

Please note that [terms and conditions apply](#).

Quantum spin liquids: a large- S route

Oleg Tchernyshyov

Department of Physics and Astronomy, Johns Hopkins University, 3400 N Charles Street,
Baltimore, MD 21218, USA

Received 7 January 2004

Published 4 March 2004

Online at stacks.iop.org/JPhysCM/16/S709 (DOI: 10.1088/0953-8984/16/11/019)

Abstract

This paper explores the large- S route to quantum disorder in the Heisenberg antiferromagnet on the pyrochlore lattice and its homologues in lower dimensions. It is shown that zero-point fluctuations of spins shape up a valence-bond solid at low temperatures for one two-dimensional lattice and a liquid with very short-range valence-bond correlations for another. A one-dimensional model demonstrates potential significance of quantum interference effects (as in Haldane's gap): the quantum melting of a valence-bond order yields different valence-bond liquids for integer and half-integer values of S .

1. Introduction

Frustrated magnets have recently become a focus of experimental studies [1–3]. Frustration disrupts long-range spin order—even at low temperatures—and leads to the formation of a spin-liquid state, in which spins move in a random yet strongly correlated fashion. A very large degeneracy of the classical ground state makes these magnets strongly susceptible to a variety of perturbations [4, 5] and thereby leads to a plethora of possible thermodynamic phases. It is also thought that the interplay of strong correlations and quantum effects may yield quantum ground states without magnetic order. Low-temperature properties of such magnets will be quite distinct from those of the familiar Bose or Fermi liquids. Therefore quantum ground states and low-energy excitations of frustrated magnets arouse considerable interest.

The ultimate example of strong frustration is the Heisenberg antiferromagnet on the pyrochlore lattice [6]. In magnets of this kind spins form a three-dimensional network of corner-sharing tetrahedra (figure 1). A nearly perfect realization of this model is found in ZnCr_2O_4 [7] where Cr^{3+} ions have spin $S = 3/2$. Recent theoretical studies of such systems have concentrated on the case $S = 1/2$ [8–13], for which the quantum effects are most prominent.

The purpose of this paper is to demonstrate viability of an alternative approach: the large- S route. There are several reasons to take this circuitous path. First, the method provides a systematic way to study quantum effects as a function of S . Second, because the very concept of a frustrated magnet is defined in the classical context, staying close to the classical limit puts

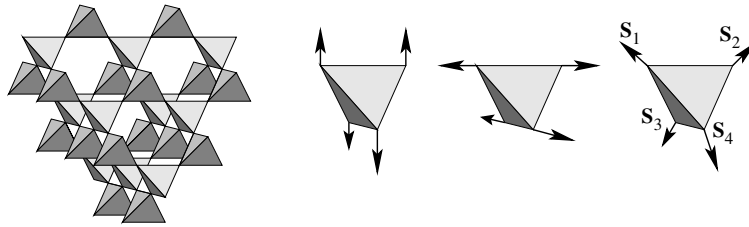


Figure 1. The pyrochlore lattice and sample ground states of Heisenberg spins on a tetrahedron.

the discussion on firmer ground. Third, magnets of this kind have a propensity toward spin-Peierls order even in the classical limit [5]. Therefore, there is a reasonable chance of finding nonclassical states—such as valence-bond solids and liquids—in pyrochlore antiferromagnets at large S .

It must be realized that the large- S problem is highly nontrivial: the starting point ($S = \infty$) has an extensive degeneracy [6]. The original problem for the three-dimensional pyrochlore lattice remains unsolved. Below we describe a few positive results that have been obtained recently for homologues of the pyrochlore antiferromagnet in one and two spatial dimensions. Section 2 outlines a degenerate perturbation theory, due to Henley, that is based on a series expansion in powers of $1/S$. To the first order in $1/S$, the theory yields a valence-bond solid for one two-dimensional ‘pyrochlore’ and a valence-bond liquid for another. By design, the *ad hoc* series expansion misses effects which are nonanalytical in $1/S$ (cf Haldane’s gap). Section 3 describes such an effect in a one-dimensional ‘pyrochlore’ chain with a spin-Peierls ground state. In that model, the quantum melting of a valence-bond solid produces qualitatively different valence-bond liquids for integer and half-integer spins.

2. A $1/S$ expansion for antiferromagnets on pyrochlore-like lattices

The starting point of the $1/S$ expansion is the limit $S \rightarrow \infty$. The ground states are found by minimizing the exchange energy $J \sum_{\langle ij \rangle} (\mathbf{S}_i \cdot \mathbf{S}_j) = \mathcal{O}(S^2)$ with respect to classical Heisenberg spin variables $\{\mathbf{S}_i\}$. In the case of the pyrochlore antiferromagnet, the total spin of every tetrahedron must vanish (figure 1). A simple counting argument [6] reveals that the manifold of classical vacua is formidably large: it contains one continuous degree of freedom per tetrahedron.

The next term in the $1/S$ expansion contains a quantum correction coming from zero-point fluctuations of spin waves [14]:

$$E^{(1)} = \text{constant} + \sum_a \frac{1}{2} \hbar \omega_a = \mathcal{O}(S), \quad (1)$$

where $\{\omega_a\}$ are spin-wave frequencies. Because magnon spectra are not the same in different ground states, the quantum correction (1) lifts the classical degeneracy. Ordinarily, quantum fluctuations select a few collinear ground states related to each other by symmetries of the lattice [15]. In some special cases, the residual degeneracy may be quite large and not linked to any obvious lattice symmetry [16].

The pyrochlore lattice presents such an exception: Henley [17] has found that an infinite number of collinear states are selected by zero-point fluctuations. These vacua are not related to each other by lattice symmetries and most are not even periodic. The exact number of degenerate ground states is not known. This accidental degeneracy has been linked by Henley to certain transformations that leave the spin-wave spectrum $\{\omega_a\}$ invariant. The transformations consist of flipping every spin on a (potentially infinite) subset of tetrahedra.

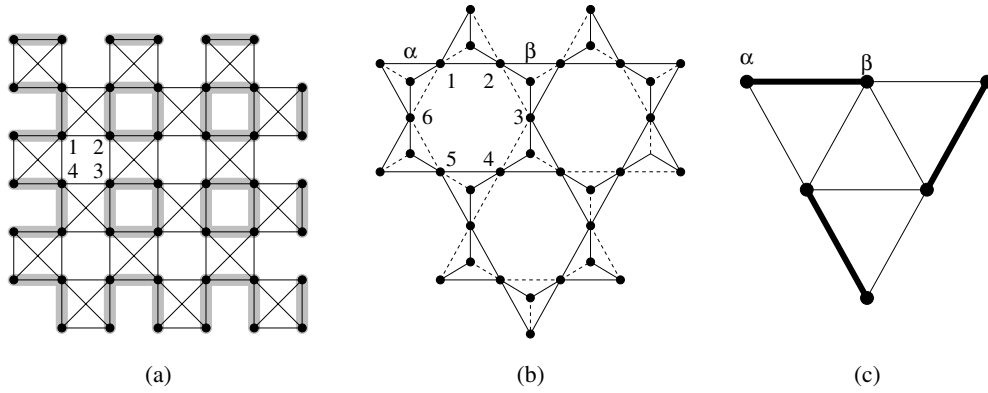


Figure 2. Two-dimensional lattices built from corner-sharing tetrahedra: (a) the checkerboard. Valence-bond order induced at low temperatures $\mathcal{O}(JS/k_B)$ is shown. $\langle \mathbf{S}_i \cdot \mathbf{S}_j \rangle = -S^2$ for the shaded bonds and zero for the rest. (b) One of the ground states of the pyrochlore wafer. Dashed lines designate frustrated bonds ($\tau_{ij} = -\sigma_i \sigma_j = -1$). (c) The dimer state that corresponds to the bond state of one sublattice of tetrahedra.

To determine which of the collinear ground states has the lowest zero-point energy, Henley has expressed the sum over the spin-wave frequencies (1) as the trace of an operator dependent on the spin values in a given ground state. The result can be expanded as an infinite sum of multi-spin potentials. In a collinear spin configuration polarized along $\hat{\mathbf{n}}$, this interaction can be expressed in terms of Ising variables $\sigma_i = (\mathbf{S}_i \cdot \hat{\mathbf{n}})/S = \pm 1$, subject to the constraint

$$\sum_{i=1}^4 \sigma_i = 0 \quad \text{on every tetrahedron.} \quad (2)$$

The zero-point energy reads [17]

$$E^{(1)} = \frac{3}{8} JS \sum_{\square} \prod_{i=1}^6 \sigma_i + \dots \quad (\text{pyrochlore lattice}). \quad (3)$$

The six-spin interaction couples spins residing around regular hexagons that exist in the pyrochlore lattice (figure 1). The omitted terms, representing multi-spin interactions of higher orders, are not necessarily small. However, at least in the two-dimensional models discussed below, their omission does not affect the selection of ground states. One can check, with the aid of Henley's symmetry, that all ground states of the truncated Hamiltonian (3) have the same zero-point energy (1).

The problem of finding the ground states thus reduces to minimizing the multi-spin interaction (3) over the Ising variables $\{\sigma_i\}$, subject to the constraint (2). It remains unsolved for the pyrochlore lattice. We have succeeded in solving it for two other lattices built from corner-sharing tetrahedra: the checkerboard and the pyrochlore wafer (figure 2). The checkerboard is a projection of the pyrochlore lattice onto a plane. Because it has loops of length 4 (around empty squares), the zero-point potential starts with four-spin interactions [17, 18]:

$$E^{(1)} = -\frac{1}{2} JS \sum_{\square} \prod_{i=1}^4 \sigma_i + \dots \quad (\text{checkerboard}). \quad (4)$$

For the pyrochlore wafer, a slice of the three-dimensional pyrochlore lattice, the effective zero-point energy is given by equation (3).

It is convenient to switch from *spin* variables σ_i to *bond* variables $\tau_{ij} = -\sigma_i\sigma_j = -(\mathbf{S}_i \cdot \mathbf{S}_j)/S^2$, defined for nearest-neighbour links ij . In terms of these, the constraint (2) requires that exactly two non-adjacent bonds be frustrated ($\tau_{ij} = -1$) on every tetrahedron. The zero-point effective potentials acquire the following form [18]:

$$-\prod_{i=1}^4 \sigma_i = -\tau_{12}\tau_{34} = -\tau_{23}\tau_{41}, \quad \prod_{i=1}^6 \sigma_i = -\tau_{12}\tau_{34}\tau_{56} = -\tau_{23}\tau_{45}\tau_{61}. \quad (5)$$

Note that the lattices in question contain two sublattices of tetrahedra and that the multi-spin interactions (5) involve bonds of tetrahedra belonging to the same sublattice—see figure 2. Thus the problem reduces to *independent* minimizations of the bond energies (5) on the two tetrahedral sublattices. Although not every bond configuration $\{\tau_{ij}\}$ corresponds to a physical spin configuration $\{\sigma_i\}$, those that minimize the bond potentials (5) do yield legitimate spin states [18].

In the checkerboard case, the bond potential (5) is minimized when every two bonds facing each other across an empty square (figure 2(a)) are in the same state (e.g. $\tau_{12} = \tau_{34} = +1$ and $\tau_{23} = \tau_{41} = -1$). The ground states of each tetrahedral sublattice fall into two disjoint classes. In one class, which can be called ‘horizontal stripes’, tetrahedra of a given row are in the same bond state. The frustrated bonds are either all vertical or all diagonal. Because every row can be in one of the two states, there are $2^{L/2}$ vacua for each sublattice. The second class—vertical stripes—is related to the first by a 90° rotation of the (sub)lattice. A more detailed derivation will be given elsewhere [18].

At zero temperature, the system is frozen in one of the striped ground states breaking the rotational symmetry of the lattice. There are two Ising order parameters: each sublattice of tetrahedra independently chooses to have vertical or horizontal stripes. The discrete nature of the order parameter guarantees survival of the long-range order at low temperatures $T < T_c$. The stripes will have a finite extent $\xi \sim \mathcal{O}(e^{a/T})$ enabling the system to move between ground states with the same orientational order on a timescale of order ξ . Thermal expectation values for the bond variables $\langle \tau_{ij} \rangle$ must therefore be averaged over all ground states with a specified orientational order. For example, when both sublattices of tetrahedra have horizontal stripes, the horizontal links always have antiparallel spins ($\langle \tau_{ij} \rangle = +1$), while all other bonds have uncorrelated spins ($\langle \tau_{ij} \rangle = 0$). Another thermal state, with horizontal and vertical stripes on the two sublattices of tetrahedra, is depicted in figure 2(a). This state has antiparallel spins around one-half of the empty squares and strongly resembles the valence-bond solid found in the ground state of the $S = 1/2$ system [11].

Apart from the number of dimensions, the checkerboard and pyrochlore lattices have one other important difference: on the checkerboard, diagonal bonds are not equivalent to vertical or horizontal ones. This is why the valence-bond order parameter on the checkerboard is of the Ising, rather than the Z_3 , type. The pyrochlore wafer (figure 2(b)) is free from this defect. What classical ground states are selected by quantum fluctuations there?

The six-spin potential (3) translates into the interaction (5) involving three bonds around a hexagon. Again, the interaction takes place between tetrahedra of the same sublattice. The three-bond energy is minimized when zero or two bonds are frustrated ($\tau_{ij} = -1$). While superficially this looks like the ground-state rule for the checkerboard, the properties of the ground states are entirely different. In particular, there is no valence-bond order. Moreover, the connected valence-bond correlations $\langle \tau_{ij}\tau_{kl} \rangle - \langle \tau_{ij} \rangle \langle \tau_{kl} \rangle$ are extremely short-ranged. This can be proven by mapping the ground states of the bond potential (5) onto classical dimer coverings of the triangular lattice, whose properties are well known [19].

The mapping is illustrated in figures 2(b) and (c). We treat the tetrahedra of one sublattice as sites of a triangular lattice. Every two tetrahedra contributing frustrated bonds to the same

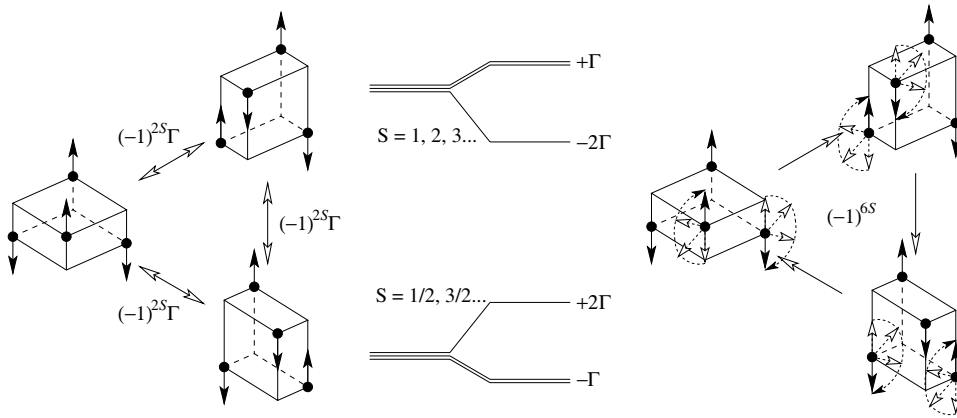


Figure 3. Tunnelling lifts the degeneracy of the three distorted ground states of spins on a tetrahedron. The ground state is a singlet for integer S and a non-Kramers doublet for half-integer S . The difference can be traced to a Berry phase acquired by the spins in a cycle of adiabatic evolution.

hexagon (such as α and β) generate a dimer linking the corresponding sites of the triangular lattice. Because each tetrahedron contributes exactly one frustrated bond to some hexagon, every site of the dual lattice is connected by a dimer to another site. For a recent update on this system see [21].

3. Nonperturbative effects: the Berry phase

To demonstrate potential significance of effects nonperturbative in $1/S$, consider a toy model of four antiferromagnetically coupled spins on a flexible tetrahedron. On a regular tetrahedron, the ground state is a spin singlet with the degeneracy $2S + 1$. A high degree of symmetry and a non-Kramers degeneracy induce the Jahn–Teller effect. For $S > 1/2$, the sum of elastic and magnetic energies is minimized by three distorted states. In each of these the ‘molecule’ is flattened along one of its principal axes (left panel of figure 3) [5].

Taking into account the kinetic energy of the atoms introduces tunnelling events between the three potential wells. The tunnelling splits the degenerate ground states into a singlet and a doublet (middle panel of figure 3). The nontrivial result is an oscillatory dependence of the order of the levels on S : the ground state is a singlet for integer spins and a non-Kramers doublet for half-integer spins.

At large S , the difference can be traced to a Berry phase acquired by the spins as the system moves between the three distorted states (the right panel of figure 3). In the process, depicting one of the potential tunnelling paths, three spins make full 2π rotations in the same plane. The overall amplitude thus acquires a geometric phase $e^{6\pi i S}$, i.e. +1 if S is integer and -1 if it is half-integer. A similar effect has been discussed by Henley and Zhang [22].

Consider now a generalization of this toy model to $d = 1 + 1$ dimensions: a chain of such tetrahedra weakly coupled through vibrational modes of the lattice (figure 4(a)). The low-energy sector of the model consists of three distorted spin-singlet ground states on each site and can be described by the quantum $q = 3$ Potts model. Elastic interactions cause the distortions of the tetrahedra to be correlated with one another. Assume, for the sake of the argument, that a uniform distortion of the chain is favoured. Then, in the absence of tunnelling, the chain has spin-Peierls order with a Z_3 order parameter. Low-energy spin-singlet excitations are domain walls with a finite energy gap Δ . As the tunnelling Γ is turned on, the spin-Peierls

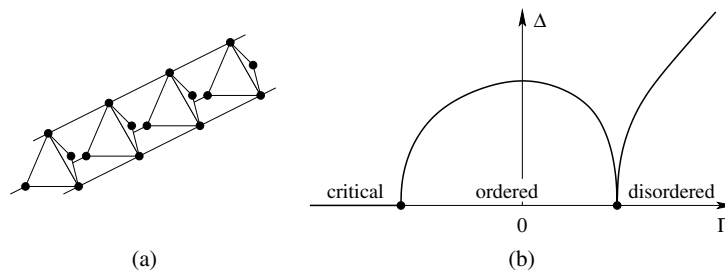


Figure 4. (a) A chain of weakly coupled tetrahedra with Heisenberg spins. For antiferromagnetic interactions, the low-energy sector consists of singlet states. (b) The phase diagram of the $q = 3$ quantum Potts model showing the energy gap for valence-bond excitations Δ as a function of the tunnelling amplitude Γ . The region $\Gamma > 0$ ($\Gamma < 0$) describes the chain with integer (half-integer) spins.

order weakens. The singlet energy gap vanishes at a quantum critical point (figure 4(b)). The nature of the quantum-disordered phase depends on the sign of the tunnelling amplitude Γ and thus on whether S is integer or half-integer.

The physics of low-energy singlet states is described by the quantum 3-state Potts model with the Hamiltonian [20]

$$H = -2 \sum_i \left[\cos\left(\frac{2\pi}{3}(\theta_{i+1} - \theta_i)\right) + \Gamma \cos\left(\frac{2\pi}{3}p_i\right) \right]. \quad (6)$$

Here $\theta_i = 0, 1, 2$ is the Potts variable, while $p_i = 0, 1, 2$ is its conjugate momentum. On the $\Gamma > 0$ side, the quantum-disordered state also has a gap to singlet excitations. For $\Gamma < 0$, the disordered state is gapless.

It is thus seen that the quantum melting of a valence-bond solid on the chain proceeds in different ways for integer and half-integer spins. The quantum-disordered phase has gapped singlet excitations when S is integer. For half-integer S , the liquid has gapless excitations in the form of valence-bond fluctuations.

References

- [1] Schiffer P and Ramirez A P 1996 *Comment. Condens. Matter Phys.* **18** 21
- [2] Harris M J and Zink M P 1996 *Mod. Phys. Lett. B* **10** 417
- [3] Greedan J E 2001 *J. Mater. Chem.* **11** 37
- [4] Moessner R 2001 *Can. J. Phys.* **79** 1283
- [5] Tchernyshyov O, Moessner R and Sondhi S L 2002 *Phys. Rev. B* **66** 064403
- [6] Moessner R and Chalker J 1998 *Phys. Rev. B* **58** 12049
- [7] Lee S H *et al* 2002 *Nature* **418** 856
- [8] Harris A B, Berlinsky A J and Bruder C 1991 *J. Appl. Phys.* **69** 5200
- [9] Canals B and Lacroix C 1998 *Phys. Rev. Lett.* **80** 2933
- [10] Koga A and Kawakami N 2001 *Phys. Rev. B* **63** 144432
- [11] Fouet J B, Mambrini M, Sindzingre P and Lhuillier C 2003 *Phys. Rev. B* **67** 054411
- [12] Tsunetsugu H 2002 *Phys. Rev. B* **65** 024415
- [13] Berg E, Altman E and Auerbach A 2003 *Phys. Rev. Lett.* **90** 147204
- [14] Henley C L 1989 *Phys. Rev. Lett.* **62** 2056
- [15] Henley C L 1987 *J. Appl. Phys.* **61** 3962
- [16] Chalker J T, Holdsworth P C W and Shender E F 1991 *Phys. Rev. Lett.* **68** 855
- [17] Henley C L 2000 unpublished
- [18] Tchernyshyov O, Starykh O A, Moessner R and Abanov A G 2003 *Phys. Rev. B* **68** 144422
- [19] Fendley P, Moessner R and Sondhi S L 2002 *Phys. Rev. B* **66** 214513
- [20] Howes S, Kadanoff L P and den Nijs M P M 1983 *Nucl. Phys. B* **215** 169
- [21] Tchernyshyov O, Yao H and Moessner R *Preprint cond-matt/0312141*
- [22] Henley C L and Zhang N G 1998 *Phys. Rev. Lett.* **81** 5221